Low-frequency noise reduction in Y-Ba-Cu-O SQUIDs by artificial defects

Peter Selders and Roger Wördenweber

Abstract — **We demonstrate, that extremely simple arrangements of few antidots in HTS rf-SQUIDs can significantly reduce the 1/f noise in ambient field down to the level of zero-field noise. The onset field B_{on}, at which the low-frequency noise starts to increase, is shifted from $B_{on}\approx 8$ μT without antidots to $B_{on}\approx 40$ μT with antidots for field cooled measurements and to $B_{on}\approx 25$ μT for zero field cooled experiments. The geometric arrangements of the antidots are obtained from the analysis of the current distribution in the washer and the position of penetrating vortices in the case of zero field cooled experiments.**

Index Terms — **antidots, low frequency noise, SQUIDs, vortex penetration**

I. Introduction

The sensitivity of cryogenic active elements is limited by the frequency dependent noise level of the device. In superconducting active devices two different sources are considered to be responsible for the noise, i.e. the contribution of the active part of the device, which usually consists of Josephson junctions, and the noise of the passive component, the superconducting thin film. Studies and understanding of the noise mechanisms in Josephson junctions are well established [1] and the noise reduction by electronical means has successfully been demonstrated [2]. The contributions of the superconducting thin film to the noise of active devices are basically understood. They are attributed to unwanted motion of quantized flux (vortices) in the superconducting thin films, which usually scales above an onset field B_{on} according to

$$\sqrt{S_\phi(f,B)} \propto \frac{B^n}{f^m} \qquad (1)$$

(f is the frequency, B the applied magnetic induction and n, m=0.5). Nevertheless, this contributions still represent a serious limitation for the application active devices especially if they are used in unshielded environment.

Various remedies to reduce the low frequency noise by vortex motion have been suggested and tested [3]-[4], which in principle can be classified into two categories: (i) either vortex penetration of the superconductor has to be avoided [3] or (ii) vortices have to be pinned by sufficiently strong pinning sites in the superconductor [4]. The first solution (flux avoidance) requires extremely small structures, e.g. narrow linewidths of w<6μm [5], which are necessary for application of these devices in ambient field up to earth field (B≈50μT). Therefore, trapping of flux by small, well positioned defects in the device would be favorable.

One of the most effective ways to create artificial pinning sites in thin films is provided by the preparation of submicrometer holes, so called antidots [6]. These defects can be placed arbitrarily in superconducting thin film devices and, in contrast to other pinning defects, which have to be of the size of the superconducting coherence length ξ, holes with sizes much larger than ξ will trap flux very effectively [7]. In previous work [7], we demonstrated that antidots can be patterned into $YBa_2Cu_3O_{7-\delta}$ (YBCO) thin films and into rf-SQUIDs without deterioration of the superconducting and SQUID properties. Commensurability effects (demonstrating the attractive interaction between vortices and antidots) and reduction of the low frequency 1/f-noise of rf-SQUIDs in ambient magnetic fields have been demonstrated [4],[7]-[8].

In this paper we demonstrate, that extremely simple arrangements of antidots in HTS rf-SQUIDs can reduce the 1/f-noise in ambient field down to the level of zero-field noise. The geometric arrangements of the antidots are motivated by analysis of the current distribution in the SQUID washer and the position of penetrating vortices. The latter can be obtained by careful analysis of the SQUID signal [13]. Different geometries of antidots are necessary for noise reduction in field-cooled (FC) experiments and in zero field cooled (ZFC) experiments. By combining the two geometries the onset field B_{on} is shifted from $B_{on}\approx 8\mu T$ without antidots to $B_{on}\approx 40\mu T$ with antidots for FC measurements and to $B_{on}\approx 25\mu T$ for ZFC experiments.

II. Experimental Setup

Planar washer type rf-SQUIDs with outer diameter of 3.5mm, SQUID holes of 100μm x 100μm and 3μm wide step-edge junction are patterned (optical lithography) and Ar ion milled into magnetron sputtered YBCO films on 2'' $LaAlO_3$ substrates. Step height and film thickness are h≈270nm and t≈320nm, respectively. Due to the wafer scaling 48 SQUIDs are fabricated simultaneously, 90% of the devices show SQUID signals with sufficiently large amplitudes of the transfer function (see Fig.1). The noise measurements are executed in liquid-nitrogen cryostat shielded with four μ-metal layers which are characterized by a residual static magnetic induction $B_{res}<5nT$. Inside the shielding ambient magnetic inductions perpendicular to the plane of the SQUIDs can be applied using Helmholtz coils with lead acid batteries as power supplies. The spectral noise density of the magnetic fields of $S_{coil}<200$ fT/√Hz

Manuscript received July 19, 2000. This work was supported in part by the DFG Grant No. WO549/3-1 and ESF scientific program VORTEX.

Peter Selders and Roger Wördenweber are with the Institute of Thin Film and Ion Technology, Research Centre Juelich, 52425 Juelich, Germany (e-mail: p.selders@fz-juelich.de, r.woerdenweber@fz-juelich.de).

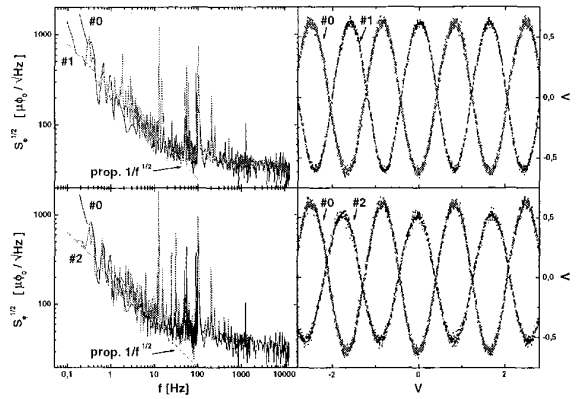

Fig. 1. Comparison of spectral noise density and transfer function of the SQUIDs before and after the additional patterning processes.

at 1Hz was for all frequencies and fields more than one magnitude smaller than the spectral noise density of the rf-SQUIDs. For most experiments the rf-SQUIDs are operated in a flux locked loop using a 600MHz rf-SQUID electronics. Due to the ac-mode of the electronics the 1/f-noise due to fluctuations in the resistance or critical current of the Josephson junction is automatically eliminated.

The field-to-flux coefficient of the SQUIDs is typically $dB/d\phi \approx 9nT/\phi_0$. The transfer function shows an amplitude of about 1.2V and a voltage to flux coefficient of about $1.65V/\phi_0$. The noise level in zero field is about 35 $\mu\phi_0/Hz^{1/2}$ ($0.3pT/Hz^{1/2}$) at 1 kHz (white noise), 200 $\mu\phi_0/Hz^{1/2}$ ($1.8pT/Hz^{1/2}$) at 1 Hz (1/f-noise), and the corner frequency lies at about 25Hz. No degradation of the SQUID performance due to the subsequent patterning of the antidots could be detected (Fig. 1).

The SQUIDs are characterized before and after the patterning processes of the different antidot configurations with respect to transfer function, spectral noise density (ZFC and FC), and penetration of vortices into the washer of the SQUID, by analyzing the unlocked SQUID-Signal. The latter is described below in more detail. These different characterization techniques provide a comprehensive set of data which allows a detailed analysis of the vortex penetration and motion in a washer type SQUID in the FC and ZFC case and their impact on the noise performance in an applied magnetic field [13].

The different SQUID configurations are (see Fig. 2):

(a) Configuration #0 represents the bare SQUID without antidots.

(b) In configuration #1 only two antidots (diameter 1.5μm) are patterned into the bare rf-SQUID (see Fig. 3).

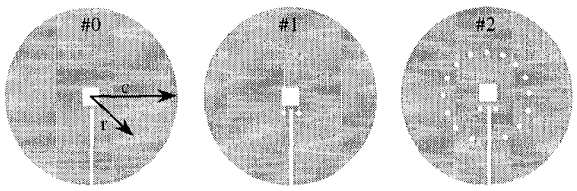

Fig. 2. Sketch of the rf SQUID with different antidot configurations: without antidots (#0), with two antidots in the vicinity of the junction (#1), and with an additional ring of antidots at r=c/2 (#2).

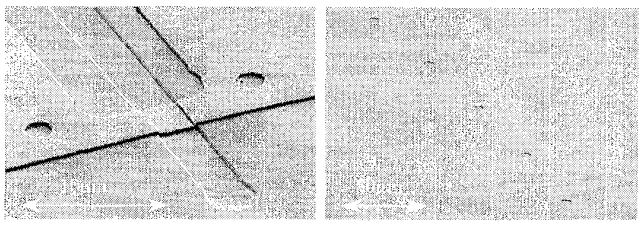

Fig. 3. SEM images of the two antidots in the vicinity of the junction (left) and the ring of antidots (right).

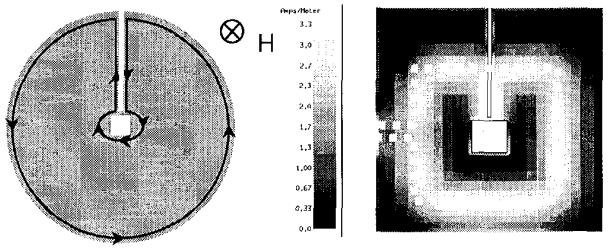

Fig. 4. Sketch of the shielding current and the result of a simulation the induced current by the rf resonant circuit. The dashed white line represents the position of the coupling coil. The current crowding close to the junction is obvious in both plots.

The position of these antidots are obtained from analyzing (i) the current distribution in the washer due to the magnetic screening and the inductively coupled rf-electronic (see Fig. 4) and (ii) the magnetic induction induced by a vortex at radial position r into the SQUID [9]. As a result of this analysis, which is given in [13], two antidots are positioned at both sides of the step-edge junction (junction-antidot center distance ≈ 8μm) in the washer (distance between the antidot center and the edge of the washer ≈ 2μm). Transfer function and noise level are not affected by the additional patterning of the antidots (Fig. 1).

(c) In configuration #2 an additional ring of antidots, positioned at r=c/2 of the circular shaped SQUID washer (see Figs. 2 and 3), is patterned into the SQUID. The optimal ring position and it's diameter are derived from the analysis of the vortex penetration in ZFC measurements and will be described below. An antidot-antidot distance of 50μm has been chosen and the diameter of the antidots is ≈ 2.5μm. Transfer function (amplitude 1.05V), voltage to flux coefficient ($1.73V/\phi_0$) and noise level at zero field are more or less not affected by the patterning process (Fig. 1).

III. Experimental Results and Discussion

In this paragraph the experimental results of FC and ZFC noise measurements and the analysis of vortex penetration into the HTS rf SQUID are presented and discussed for the different configurations.

A. Field cooled (FC) noise measurements

Independent of the applied inductions and the configuration the FC measurements generally revealed 1/f-type noise spectra at low frequencies. A 1/f noise spectrum in HTS films is generally ascribed to an incoherent superposition of many

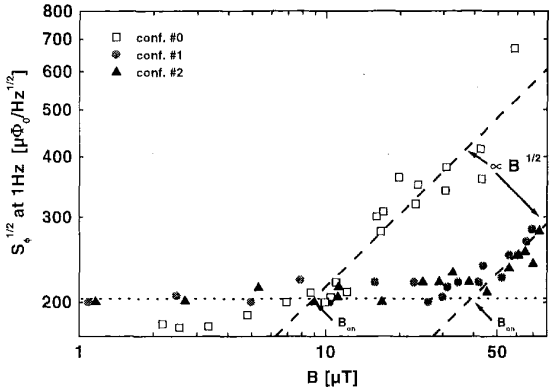

Fig. 5. Spectral noise density obtained for FC measurements at 1 Hz as function of the applied magnetic induction B for rf-SQUIDs with different configurations of antidots. Each data point represents an average value obtained from independent FC measurements.

microscopic fluctuators, i.e. thermally activated vortices with a distribution of activation energies for vortex hopping processes [9].

A comparison of the spectral noise density in the 1/f-regime of all configurations is given in Fig. 5. Each data point represents an average value obtained from independent FC measurements. The double logarithmic plot of $S_\phi^{1/2}$ at 1Hz as function of B shows the following features:

(i) At low fields ($B<B_{on}$) $S_\Phi^{1/2}\approx 180\text{-}200\mu\phi_0/Hz^{1/2}$ is identical for all configurations and independent of the applied field.

(ii) At high fields ($B>B_{on}$) the spectral noise densities increase with increasing field according to the theoretical expectation given in eq. (1).

(iii) However, the transition from the field independent to the field dependent spectral noise density is strongly shifted from $B_{on}\approx 8\mu T$ without antidots (conf. #0) to $B_{on}\approx 40\mu T$ with antidots (conf. #1 and #2).

The increase of the onset field B_{on} by the arrangement of antidots has been discussed in parts in [8]. The low-frequency noise is dominated by motion of vortices in the superconducting film, which are close to the SQUID hole. In this area a crowding of shielding and induced (by the rf resonant circuit) currents; which is expected to add to the activation of vortices, is observed in the vicinity of the junction (Fig. 4). Since the stripline on which the junction is positioned is too small (3μm) to contain vortices, antidots, which act as pinning sites for the vortices, are most efficient in noise reduction if they are placed close to the junction. This is exactly, what we observe in the experiment. The onset field is strongly enhanced due to the additional two antidots, whereas the additional antidot ring (conf. #2) did not lead to a further improvement of the FC noise spectra.

B. Zero field cooled measurements

In the following ZFC measurements of the low frequency noise and the penetration of vortices into the washer are presented. The latter will be discussed in details in [13]. The analysis of vortex penetration motivates the position of the additional antidots of conf. #2, which is optimized for ZFC experiments.

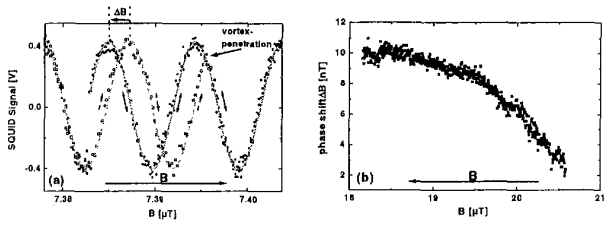

Fig. 6. (a) Discrete phase shift of the unlocked SQUID Signal due to a penetrating vortex. (b) Diffusion like motion of a vortex in the washer.

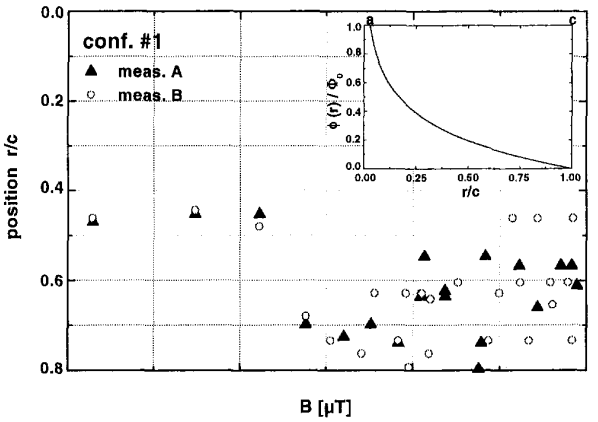

Fig. 7. Positions of the penetrated vortices in conf. #1. The inset shows the position dependent coupling of a vortex into the SQUID.

Discontinuities of the unlocked SQUID signal (see typical example in Fig. 6(a)) are caused by the penetration of vortices into or expulsion of vortices out of the washer. In contrast to the diffusion like motion of vortices within the washer (Fig. 6(b)) [13], in this case the vortex has to overcome the surface barrier at the edge of the washer [10]-[11]. The resulting phase shift in the SQUID signal is correlated to a change ΔB of magnetic induction in the SQUID, which yields information about the radial position of the vortex after penetration. The dependent fraction ϕ(r) of the flux quantum which couples into the SQUID hole as function of the radial position of a vortex is displayed in the inset of Fig. 7 [9]. Thus; using the field-to-flux coefficient $dB/d\phi$, the discrete phase shifts, which are observed in ZFC experiments, can be transformed into discrete flux changes Δϕ. Fig. 7 displays the resulting positions of the penetrated vortices for two independent measurements and conf. #1. Two different field regimes can be distinguished. For small inductions $B<13\mu T$ only a few (i.e. 3) vortices penetrate the washer. Magnetic fields and positions of penetration are reproducible. The radial position of the first 3 vortices is given by $r=c/2$, which therefore was chosen for the position of the additional antidot ring in conf. #2. At higher applied magnetic inductions $B>13\mu T$ the penetration starts to become more statistical. Induction and position of the penetrating vortices are not reproducible anymore. Nevertheless the total number of penetrating vortices is quite similar for all configurations (see Fig. 8b).

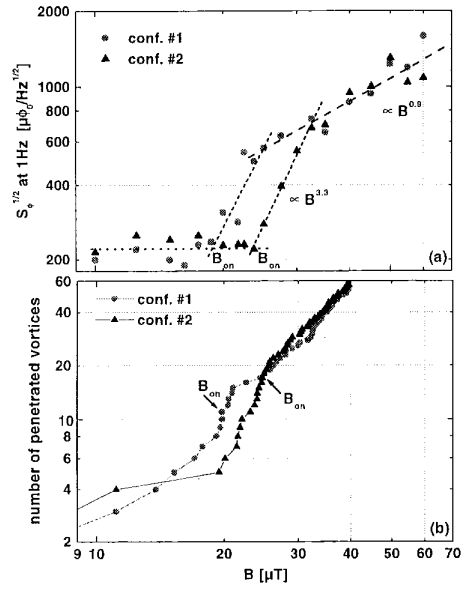

Fig. 8. Spectral noise density in ZFC measurements at 1 Hz and the number of penetrating vortices as a function of the applied magnetic induction. The antidot configurations #1 and #2 are compared. The coincidence of the onset of the increase of the low frequency noise at 1 Hz and the increasing number of penetrating vortices is visible. In configuration #2 is the penetration of the vortices delayed and therefore the onset of the noise increase is shifted by the introduction of the antidot ring from 18μT (conf. #1) to 25μT (conf. #2)

The improvement of the ZFC noise data obtained by the additional antidot ring is demonstrated in Fig. 8. For both antidot configurations an initial steep increase ($B \propto B^{3.3}$) of the low frequency noise at B_{on} is detected which becomes smoother ($B \propto B^{0.9}$) at higher magnetic inductions. This unusually steep increase of S_ϕ is a consequence of the small number of penetrating vortices, which automatically implies a large difference between the applied and the penetrated field. However, due to the introduction of the antidot ring the first penetrating vortices seem to be pinned and the penetration of the successive vortices which seem to be related to the increase of the low frequency noise in conf. #1 is delayed. This results in a increase of the onset field from $B_{on} \approx 18\mu T$ for conf. #1 to $B_{on} \approx 25\mu T$ for conf. #2. Finally, the total number of penetrating vortices is similar for both configurations (Fig. 8b). It demonstrates, that the onset of the increase of low-frequency noise does not depend on the number of penetrating vortices. The onset takes place for about 10 vortices for conf. #1, whereas about 19 vortices have penetrated the washer in conf. #2 before the onset is observed.

IV. Conclusions

In conclusion, we demonstrated that (i) quite simple arrangements of a few antidots can lead to significant reduction of the low-frequency noise in HTS SQUIDs in ambient fields and (ii) that a careful analysis of the SQUID signal can be used to identify the position of the first penetrating vortices. Patterning only two antidots in the vicinity of the Josephson junction and a ring of antidots at the position of the first penetrating vortices (here: $r=c/2$) the onset field, at which the low-frequency noise starts to increase, is shifted from $B_{on} \approx 8\mu T$ without antidots to $B_{on} \approx 40\mu T$ in FC measurements and to $B_{on} \approx 25\mu T$ in ZFC measurements. The analysis of the vortex penetration was used to identify the position of the antidots. Finally, the improvement of the relatively simple superconducting device demonstrated the potential of antidots in applications. Further improvements of the field stability of HTS SQUIDs or the improvement of other active superconducting devices by specially positioned antidots seem to be possible and should be tested in the future.

Acknowledgment

The authors like to acknowledge H.P. Bochem, A.I. Braginski, S. Bunte, A. Castellanos, R. Gross, N. Klein, R. Kleiner, D. Koelle, R. Kutzner, P. Lahl, R. Ott, R. Straub and M. Vaupel.

References

[1] R. Gross and B. Mayer, Physica C, vol. 180, pp. 235, 1991, M. Kawasaki, P. Chaudhari, and A. Gupta, Phys. Rev.. Lett., vol. 68, pp. 1065, 1992, A. Marx, and R. Gross, Appl. Phys. Lett., vol. 70, pp. 120, 1997, A. H. Miklich, J. Clarke, M. S. Colclough, and K. Char, Appl. Phys. Lett., vol. 60, pp. 1899, 1992.

[2] R. L. Forgacs, and A. F. Warwick, Rev. Sci. Instrum., vol. 38, pp. 214, 1967, V. Foglietti et al., Appl. Phys. Lett., vol.49, pp. 1393, 1986, R. H. Koch et al., J. Low Temp. Phys., vol. 51, pp. 207, 1983, R. H. Koch et al., Appl. Phys. Lett., vol. 60, pp. 507, 1992, A. H. Miklich et al., IEEE Trans. Appl. Supercond., vol. 3, pp. 2434, 1993, M. Mück, C. Heiden, and J. Clarke, J. Appl. Phys., vol. 75, pp. 4588, 1994.

[3] E. Dantsker, S. Tanaka, and J. Clarke, Appl. Phys. Lett., vol. 70, pp. 2037, 1997, R.H. Koch, J. Z. Sun, V. Foglietta, and W. J. Gallagher, Appl. Phys. Lett., vol. 67, pp. 709, 1995.

[4] T. J. Shaw, J.Clarke, R. B. van Dover, L. F. Schneemeyer, and A. E. White, Phys. Rev. B, vol. 54, pp. 15411, 1996, P. Selders, A. Castellanos, M. Vaupel, and R. Wördenweber, Appl. Supercond., vol. 5, pp. 269, 1998.

[5] J. R. Clem, "Vortex exclusion from superconducting strips and SQUIDs in weak perpendicular ambient magnetic fields," unpublished.

[6] M. Baert, V. V. Metlushko, R. Jonckheere, V. V. Moshchalkov, and Y. Bruynseraede, Phys. Rev. Lett., vol. 74, pp. 3269, 1995, A. N. Lykov, Sol. St. Comm., vol. 86, pp. 531 1993.

[7] A. Castellanos, R. Wördenweber, G. Ockenfuss, A. v.d. Hart, and K. Keck, Appl. Phys. Lett., vol. 71, pp. 962, 1997, R. Wördenweber, A. M. Castellanos, and P. Selders, Physica C, vol. 332, pp. 27, 2000.

[8] P. Selders and R. Wördenweber, Appl. Phys. Lett., vol. 76, pp. 3277, 2000.

[9] M.J. Ferrari et al., J. Low Temp. Phys., vol. 94, pp. 15, 1994.

[10] C. P. Bean and J. D. Livingston, Phys. Rev. Lett., vol. 12, pp. 14, 1964.

[11] E. Zeldov et al., Phys. Rev. Lett., vol 73, pp. 1428, 1994.

[12] M.J. Ferrari, J.J. Kingston, F.C. Wellstood, and J. Clarke, Appl. Phys. Lett., vol. 58, pp. 1106, 1991.

[13] P. Selders and R. Wördenweber, "Magnetic field behavior of $YBa_2Cu_3O_{7-\delta}$ Superconducting Quantum Interference Devices with antidots," unpublished.